CHARACTERISTICS OF THREE-DEMENSIONAL STRONG GROUND MOTIONS ALONG PRINCIPAL AXES

Bunho KOJIKA[1], Keiichi OHTANI[2] And Tsuneo KATAYAMA[3]

SUMMARY

Analysis of three-dimensional strong ground motions along principal axes was carried out based on K-NET records. By applying moving window technique to ground motion records, the time-dependent characteristics of ground motions along principal axes were examined. It is observed that the three rotation angles between conventional coordinates and principal axes are the function of time and the angles keep stable for a short time period after the arrivals of P and S waves, respectively. This indicates that the directly arrived P and S waves have their respective specific input directions. The rotation angle around vertical axis is almost zero after S wave arrives, which means that the principal axes vary only in horizontal plane after S wave arrives. Mean rotation angle was calculated for the stable time period after the arrival of S wave. Making use of the mean rotation angle and the maximum variance along principal axes of all observation stations, the spatial distribution characteristics of principal axes was investigated. A clear relationship between the two horizontal principal directions and the direction of source was not found.

On the other hand, although the radiation patterns of SH and SV waves have a simple form of **sin**(2φ) and **cos**(2φ), respectively, in the moment release plane, they become very complicated in horizontal plane for general source mechanism. With the source mechanism of earthquakes, the theoretical solutions of SH and SV waves were obtained. Under the assumption of horizontal layer structure, the vibration directions of SH and SV waves are transverse and radial with respect to source direction, respectively. Because SH and SV waves share the same source spectrum and ray path, the correlation between SH and SV waves exists and the principal axes of SH and SV waves can be obtained theoretically. The results of principal axes based on theory and that based on observation data were compared.

INTRODUCTION

Shaking table test provides a powerful means to investigate the complicated mechanism of the failure of structures under three-dimensional earthquake loads. However, the ground motion records with large magnitude and short focal distance, which are often required as the input of shaking table, are very limited. As the first step to estimate the three-dimensional ground motion input for shaking table test, the characteristics of the three-dimensional ground motions along principal axes and their relationships with the source mechanism, direction from site to source were examined in this paper.

According to the recent studies from the strong ground motions of large earthquakes such as 1994 Northridge earthquake and 1995 Kobe earthquake, it becomes clear that the correlation of three-dimensional ground motions have a considerable influence on the failure of structures. The purpose of this paper is to elucidate the correlation between the three-dimensional ground motions through an analysis of strong motion records. The strong ground motions recorded by K-NET (a strong ground motion observation network in Japan with an distance of about 25 km between stations), which can be accessed over Internet, were used here. Forty

[1] *National Research Institute for Earth Science and Disaster Prevention, STA, Japan, Email: kojika@ess.bosai.go.jp*
[2] *National Research Institute for Earth Science and Disaster Prevention, STA, Japan, Email:ohtani@knetgk.k-net.bosai.go.jp*
[3] *National Research Institute for Earth Science and Disaster Prevention, STA, Japan, Email: katayama@ess.bosai.go.jp*

earthquakes whose magnitude is larger than 5.0 and the maximum acceleration exceeds 100 gal were selected from the K-NET database. The parameters of selected earthquakes are shown in Table 1. For each selected earthquake, at least several tens of observation records are available.

Table 1: The list of selected earthquakes

No.	Original time	M(JMA)	Depth	Lat., Long.
1	1996/05/23 18:36	5.0	39 km	38.7˚, 142.3˚
2	1996/08/11 03:12	5.9	10 km	38.9˚, 140.6˚
3	1996/09/09 13:34	5.7	20 km	30.5˚, 130.9˚
4	1996/10/19 23:44	6.6	39 km	31.8˚, 132.0˚
5	1996/12/21 10:29	5.4	53 km	36.1˚, 139.9˚
6	1997/02/20 05:22	5.4	90 km	37.4˚, 141.2˚
7	1997/02/20 16:55	5.6	50 km	41.8˚, 142.9˚
8	1997/03/03 23:09	5.0	3 km	35.0˚, 139.2˚
9	1997/03/04 12:51	5.7	2 km	35.0˚, 139.2˚
10	1997/03/16 14:51	5.8	39 km	34.9˚, 137.5˚
11	1997/03/26 17:31	6.3	8 km	32.0˚, 130.4˚
12	1997/04/03 04:33	5.5	9 km	32.0˚, 130.3˚
13	1997/05/12 07:59	5.5	54 km	37.0˚, 141.3˚
14	1997/05/13 14:38	6.2	8 km	32.0˚, 130.3˚
15	1997/05/18 06:25	5.0	10 km	32.4˚, 130.6˚
16	1997/06/15 13:54	5.1	100 km	43.0˚, 144.2˚
17	1997/06/25 18:50	6.1	12 km	34.5˚, 131.7˚
18	1997/09/04 05:16	5.2	6 km	35.3˚, 133.4˚
19	1997/10/11 14:44	5.0	30 km	34.4˚, 138.2˚
20	1997/11/15 16:05	6.1	153 km	43.7˚, 145.1˚
21	1997/12/07 12:50	5.3	83 km	37.7˚, 141.8˚
22	1998/01/03 03:20	5.3	50 km	42.9˚, 145.5˚
23	1998/02/21 09:55	5.0	21 km	37.3˚, 138.8˚
24	1998/04/09 17:45	5.4	93 km	36.9˚, 141.0˚
25	1998/04/22 20:32	5.4	10 km	35.2˚, 136.6˚
26	1998/05/03 11:09	5.7	3 km	35.0˚, 139.2˚
27	1998/05/21 06:54	5.0	84 km	38.6˚, 142.1˚
28	1998/05/23 04:49	5.3	85 km	33.7˚, 131.9˚
29	1998/08/16 03:31	5.4	5 km	36.3˚, 137.6˚
30	1998/08/29 08:46	5.1	67 km	35.6˚, 140.1˚
31	1998/09/03 16:58	6.1	10 km	39.8˚, 140.9˚
32	1998/09/15 16:24	5.0	13 km	38.3˚, 140.8˚
33	1998/11/24 04:48	5.1	82 km	38.0˚, 141.6˚
34	1999/01/24 09:37	5.9	50 km	30.6˚, 131.3˚
35	1999/02/26 14:18	5.1	19 km	39.2˚, 139.9˚
36	1999/03/11 20:06	5.0	40 km	39.6˚, 141.9˚
37	1999/03/16 16:43	5.1	10 km	35.3˚, 135.9˚
38	1999/03/26 08:31	5.1	50 km	36.5˚, 140.6˚
39	1999/04/25 21:27	5.2	50 km	36.5˚, 140.5˚
40	1999/05/13 02:59	6.1	100 km	43.0˚, 143.9˚

ANALYSIS METHOD

The three components of ground motion records represent, in general, the accelerations measured along the instrument axes. If ground motions are assumed to be Gaussian stochastic process with zero mean values, the three-dimensional ground motion process can be completely characterized in a probabilistic sense through the covariance matrix

$$c(t,\tau) = \begin{bmatrix} c_{xx} & c_{xy} & c_{xz} \\ c_{yx} & c_{yy} & c_{yz} \\ c_{zx} & c_{zy} & c_{zz} \end{bmatrix} \tag{1}$$

where

$$c_{ij} = c_{ij}(t,\tau) = E\left[a_i(t)a_j(t+\tau)\right], \quad i, j = x, y, z \tag{2}$$

and **E** denotes the ensemble average. In this case, the influence of coordinate directions in the covariance functions in Equation (1) can be investigated through the approximate relations [Kubo and Penzien, 1979]

$$c_{ij}(t,0) = E\left[a_i(t)a_j(t)\right], \quad i, j = x, y, z \tag{3}$$

The components of motion along orthogonal axes x', y', z' can be simply transformed to components along another orthogonal axes x, y, z by

$$\begin{Bmatrix} a_x(t) \\ a_y(t) \\ a_z(t) \end{Bmatrix} = A \begin{Bmatrix} a_{x'}(t) \\ a_{y'}(t) \\ a_{z'}(t) \end{Bmatrix} \tag{4}$$

where **A** is a transformation matrix satisfying the condition

$$A^T A = I \text{ (Identity matrix)} \tag{5}$$

Then the covariance matrix for axes x', y', z' is

$$c'(t) = A^{-1}c(t)\left(A^{-1}\right)^T$$

$$= A^T c(t) A \tag{6}$$

This transformation of three-dimensional ground motion is identical to that of three-dimensional state of stress. Therefore, A set of principal axes exists along which the components of ground motion have maximum, minimum and intermediate values of variance and have zero values of covariance. It can be easily shown that the directions of the principal axes are the eigenvectors derived through the use of the covariance matrix defined be Equation (1) and the principal variances are the corresponding eigenvalues, i.e.

$$c_P(t) = P^T c(t) P$$

or

$$c_P(t) = \begin{bmatrix} c_{11}(t) & 0 & 0 \\ 0 & c_{22}(t) & 0 \\ 0 & 0 & c_{33}(t) \end{bmatrix} \tag{7}$$

Where **P** is an orthogonal matrix which designates the principal transformation matrix.

Since the off-diagonal terms in a covariance matrix indicate quantitatively the correlation between the corresponding components, the components along the principal axes are fully uncorrelated with respect to each other. For Gaussian stochastic processes, they are statistically independent of each other if they are uncorrelated with each other. Therefore, the components directed along principal axes are independent of each other in a statistical sense.

In practical application, the desired properties of stochastic processes can often be estimated by examining individual members from the processes if assuming the process is an ergodic process.

CHARACTERISTICS OF GROUND MOTIONS ALONG PRINCIPAL AXES

Because ground motions are non-stationary, a moving window technique was applied in order to see the time-varying characteristics. The principal axes of ground motion are defined by the three rotation angles of r_x, r_y and r_z to satisfy equation (7). r_x, r_y and r_z are the rotation angles with respect to x, y and z axes, respectively.

From principal axis analysis, some of which are shown in Figures 1 and 2, the findings are summarized as follows:

1. The three rotation angles of r_x, r_y and r_z are time dependent, but they are stable for a short time period after the arrival time (T_P and T_S) of P and S waves, respectively. This indicates that the direct P and S waves have their respective specific input directions.
2. The rotation angles r_x and r_y are nearly zero after S wave arrives. This means the principal axes vary only in horizontal plane after S wave arrives. This can also be shown by comparing it with the rotation angle r_2, which is the transformation function from X and Y coordinates to principal axes in horizontal plane.
3. The directions of the two principal axes in horizontal plane were examined by the mean rotation angles of the stable time period after the arrival of S wave for all of the observation stations. A close relationship between the directions of principal axes and the direction of source was not found.

From the spatial distribution of the maximum and intermediate principal axes, their correlation with radiation pattern of SH and SV waves was not found, either.

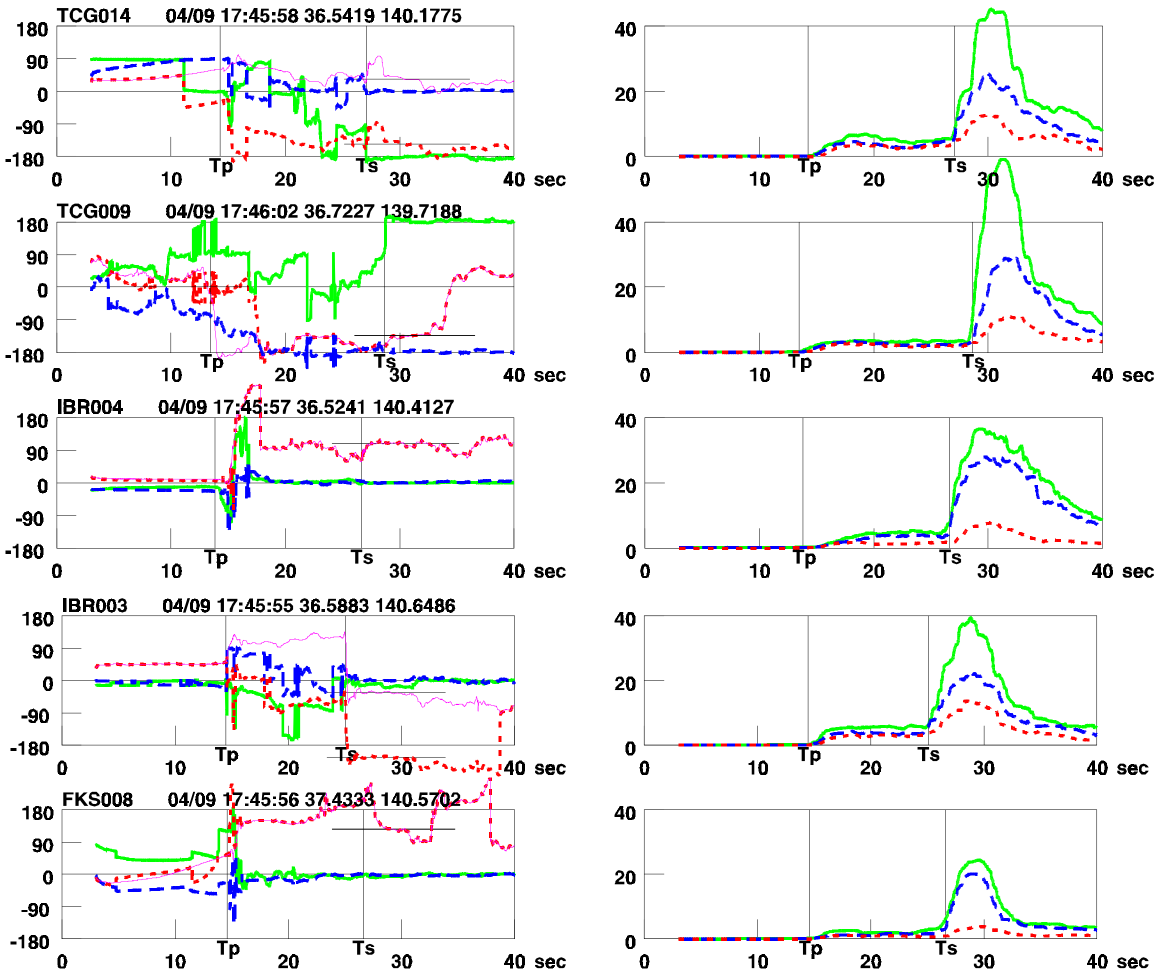

(a) Rotation angles of principal axes **(b) Square root of principal variances**

r_x: ——, r_y: – – , r_z: ⋯⋯, r_2: —— σ_1: ——, σ_2: – – , σ_3: ⋯⋯

Figure 1: Rotation angles of principal axes and the square root of principal variances.

(M5.4, Depth93km, 1998/04/09 17:45)

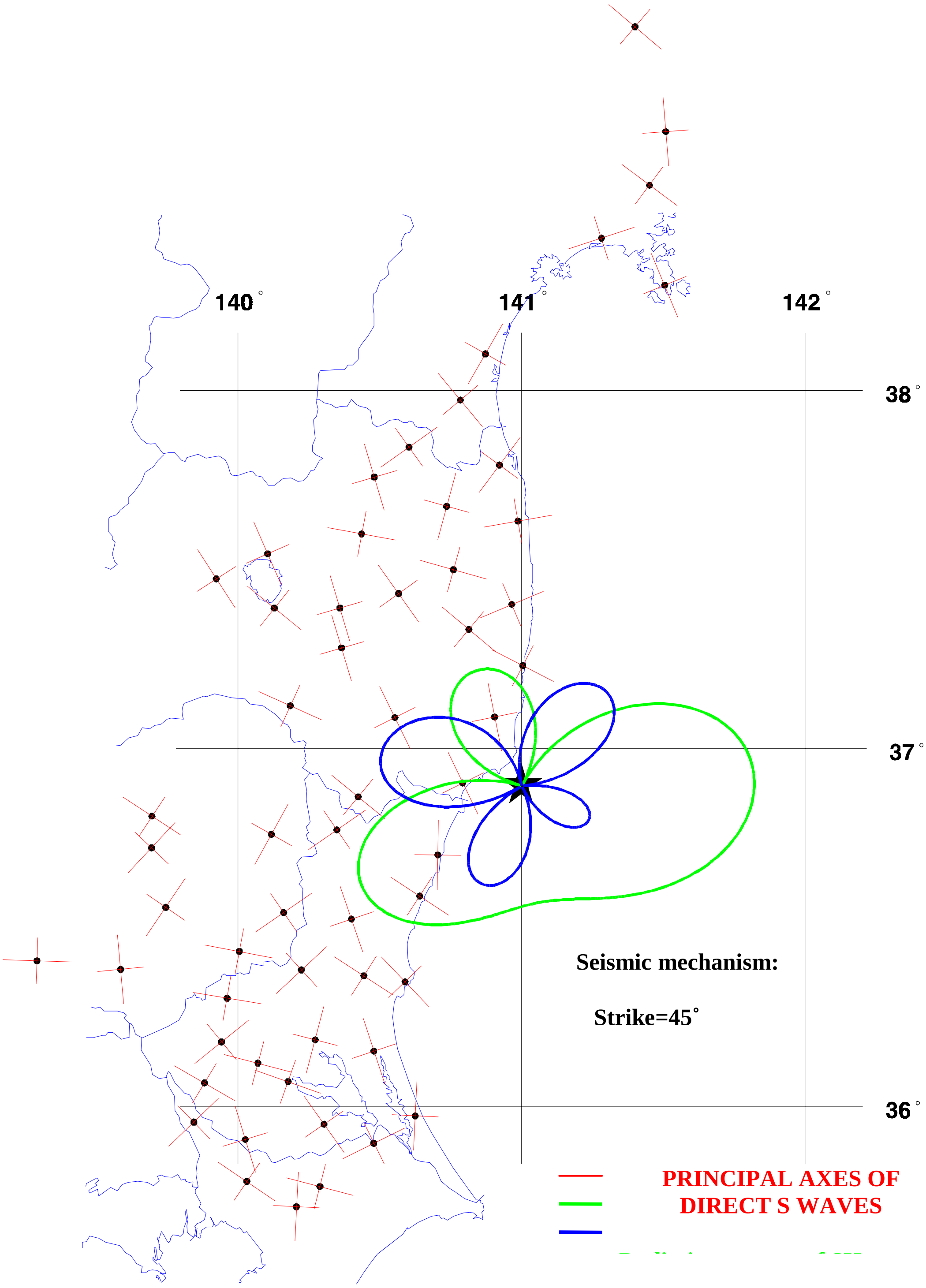

Figure 2: Distribution of principal axes of direct S wave and radiation pattern of SH and SV waves. (M5.4, Depth93km, 1998/04/09 17:45)

INFLUNENCE OF SOURCE MECHANISM

When the source mechanism of an earthquake is known, the SH wave and SV wave can be theoretically calculated. The SH and SV waves have the same source spectrum and the same path from source to site. The only difference between them is their radiation pattern. In this regard, SH wave and SV wave should be resemblance to each other and there exists a predominant axis for SH and SV waves. S wave vibrates in the shaft direction of the predominant axis only. The vibration amplitude is zero in the plumb direction. The predominant direction can be determined by the equation

$$c_{m_1 m_2} = \frac{1}{2\pi} \int_{-\infty}^{\infty} F_{m_1}(\omega) F_{m_2}(\omega) d\omega = 0 \tag{8}$$

with coordinates transformation

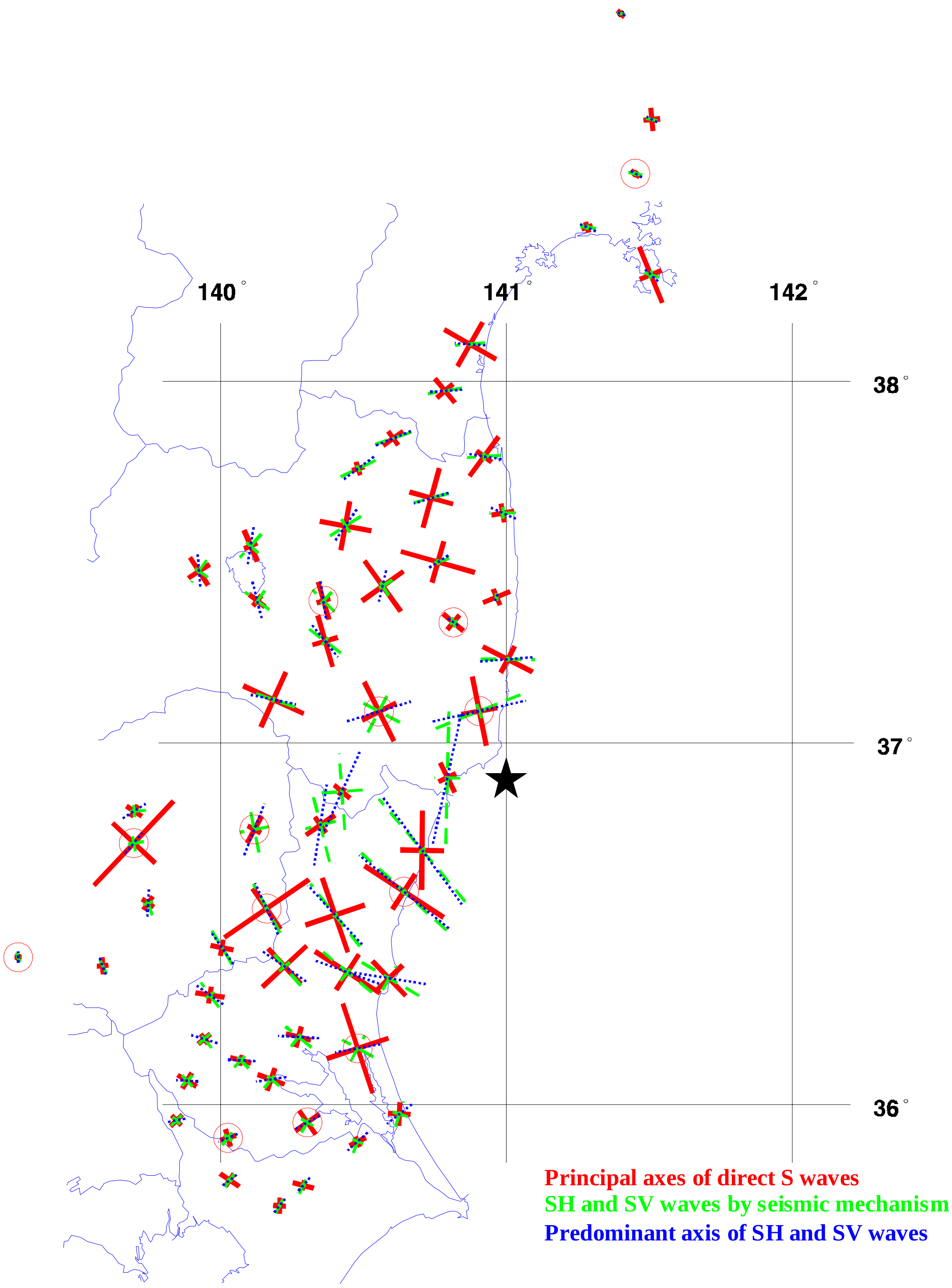

Figure 3: Comparison of the direction and amplitude of principal axes, SH and SV waves, and the predominant axis of SH and SV wave. (M5.4, Depth93km, 1998/04/09 17:45)

$$
\begin{aligned}
m_1 &= \quad SV \cdot \cos\theta_m + SH \cdot \sin\theta_m \\
m_2 &= -SV \cdot \sin\theta_m + SH \cdot \cos\theta_m
\end{aligned}
\tag{9}
$$

and

$$
\begin{aligned}
F_{SV}(\omega) &= R_{SV} \cdot S_{ource}(\omega) \cdot P_{ath}(\omega) \\
F_{SH}(\omega) &= R_{SH} \cdot S_{ource}(\omega) \cdot P_{ath}(\omega)
\end{aligned}
\tag{10}
$$

where $S_{ource}(\omega)$ is source spectrum of S wave, $P_{ath}(\omega)$ is path effects and R_{SV} and R_{SH} are radiation patterns of SV and SH waves, respectively. Substitute Equations (9) and (10) into Equation (5), the rotation angle θ_m, from which the predominant axis is determined, can be derived.

$$
\theta_m = \frac{1}{2}\tan^{-1}\left(\frac{2R_{SV}R_{SH}}{R_{SV}^2 - R_{SH}^2}\right) \tag{11}
$$

The principal axes and amplitudes of S wave from the observed ground motions, the amplitudes of SH and SV waves of the theoretical solution from the source mechanism, and the predominant axis of SH and SV waves are compared in Figure 3. When the difference of the directions of principal axes and predominant axis for a site is less than 10 degrees, it is marked with a red circle. The red-marked sites are about 20% of the total observation sites.

From the theoretical solution of source mechanism, SH wave and SV wave are completely correlated and they can be composed to a vector in the predominant axis. On the other hand, it is found that the vibration along the maximum principal axis is not so larger than that along the minimum principal axis from ground motion records. The principal axis analysis of ground motions in short period range cannot explain the theoretical solutions of SH and SV waves.

CONCLUSIONS

The principal axes of ground motions were calculated by zeroing the all covariance values of the covariance matrix of the three components of ground motion records. The principal axes are time varying in general, but after arrivals of P and S waves, a respective stable time period of several seconds is observed. This means that the direct P wave and the direct S wave have their respective specific input directions. The principal axes for direct S wave was compared with the theoretical solution of SH and SV waves from source mechanism, the correlation between them is not found. For theoretical solution, because SH and SV waves share a common source spectrum and have the same path, the different radiation pattern between them results in that SH and SV waves are completely correlated and they can be composed to a vector in ground surface. The S wave of ground motion cannot be composed to a vector in horizontal plane. There are about 20% sites where the difference between the directions of the vector and the principal axes is within 10 degrees. The theoretical solution of SH and SV waves, which is obtained by the horizontal layer assumption, cannot explain the principal axes analysis results of the short period ground motions.

REFERENCES

Kubo, T. and J. Penzien (1979), "Analysis of three-dimensional strong ground motions along principal axes, San Fernando earthquake", *Earthquake Engineering and Structure Dynamics*, Vol.7, pp.265-278.